


LETTER TO EDITOR

Hindering triple negative breast cancer progression by targeting endogenous interleukin-30 requires IFN γ signaling

Carlo Sorrentino^{1,2} | Stefania Livia Ciummo^{1,2} | Luigi D'Antonio^{1,2} | Paola Lanuti¹ | Scott I. Abrams³ | Zhinan Yin⁴ | Li-Fan Lu⁵ | Emma Di Carlo^{1,2} 

¹ Department of Medicine and Sciences of Aging, "G. d'Annunzio" University, Chieti, Italy

² Anatomic Pathology and Immuno-Oncology Unit, Center for Advanced Studies and Technology (CAST), "G. d'Annunzio" University, Chieti, Italy

³ Department of Immunology, Roswell Park Cancer Institute (RPCI), Buffalo, New York, USA

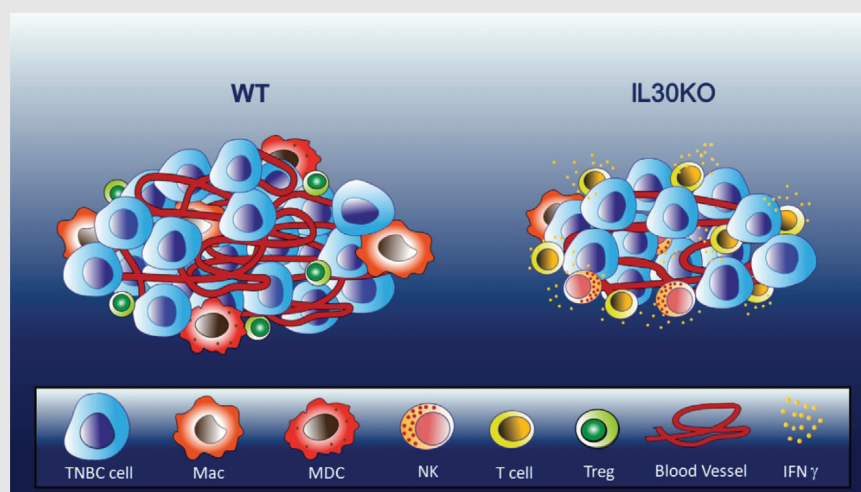
⁴ The First Affiliated Hospital, Biomedical Translational Research Institute, Guangdong Province Key Laboratory of Molecular Immunology and Antibody Engineering, Jinan University, Guangzhou, China

⁵ Division of Biological Sciences, Center for Microbiome Innovation and Moores Cancer Center, University of California, San Diego, California, USA

Correspondence

Emma Di Carlo, Anatomic Pathology and Immuno-Oncology Unit, Center for Advanced Studies and Technology (CAST), "G. d'Annunzio" University, Via L. Polacchi 11, 66100, Chieti, Italy.
Email: edicarlo@unich.it

Graphical Abstract



- IL30mRNA expression is associated with the TNBC subtype.
- IL30 boosts proliferation and migration of TNBC cells and reshapes their immunity gene expression profile.
- The lack of endogenous IL30 hinders TNBC growth and progression and prolongs host survival.
- TNBC growth inhibition, due to the lack of endogenous IL30, requires IFN γ production by T and NK cells.

LETTER TO EDITOR

Hindering triple negative breast cancer progression by targeting endogenous interleukin-30 requires IFN γ signaling

Dear Editor,

We recently identified interleukin (IL) 30 as a chief regulator of prostate and breast cancer (BC) microenvironments.^{1,2,3} Produced by cancer and infiltrating myeloid-derived cells (MDC), IL30 primes transcriptional activation of oncogenes and metastasis-related genes and promotes cancer stem-like cell proliferation and migration, driving tumor progression.

Identified as a partner of the Epstein-Barr virus-induced gene 3 (EBI3) to form the heterodimeric cytokine IL27,⁴ IL30 can behave as a self-standing cytokine, which signals via IL6R α (CD126) by recruiting a gp130 (CD130) homodimer.⁵

IL30 expression by tumor- and draining lymph node (LN)-infiltrating leukocytes, is frequent in triple-negative (TN) BC, one of the deadliest malignancies, and has been associated with recurrence and worse overall survival.³

Bioinformatic analyses of microarray data, obtained from 1699 BC cases included in the METABRIC cohort (Supplementary Methods), established a positive correlation between *IL30*mRNA expression and TNBC, versus Luminal A ($P < .0001$), versus Luminal B ($P = .045$) and versus Normal-like ($P = .047$) BCs (Figure 1A). Expression of *IL30*mRNA in HER2⁺BC was comparable to that of TNBC and significantly ($P < .001$) higher than in Luminal A, whereas no difference was found between the remaining BC subtypes. Although the prevalence of TNBC (15–20% of all BCs) may seem low, the high incidence of BC, estimated at 2 000 000 cases per year worldwide,⁶ means that ~30 000 patients (7.54% of TNBCs) will be newly diagnosed with IL30⁺ TNBCs each year. Since IL30 expression also involves 5% of HER2⁺ (10 000 cases), 3.47% of Luminal B (12 000 cases), 2.14% of Normal-like (2 000 cases), and 0.74% of Luminal A (6 000 cases) BCs, the total number of patients with IL30⁺ BCs will be ~60,000.

To find out whether IL30 targeting in the host environment might affect TNBC behavior, murine TNBC cell lines,

E0771, and AT-3, were first tested for their responsiveness to IL30 and then implanted into syngeneic, *EIIa-p28^{fl/fl}*, IL30 conditional knockout⁷ (*IL30KO*) hosts (Supplementary Methods).

Only E0771 cells expressed both IL30 receptor (R) chains (Figures 1B and 1C; Figure S1 and Supplementary Methods). Both cell lines did not release IL30, which excludes autocrine effects. AT-3 cells proved unresponsive to rmIL30 in proliferation and motility tests (Figures 1D and 1E), and immunity gene expression profiling. By contrast, rmIL30 increased proliferation (ANOVA: $P < .001$) and migration (ANOVA: $P = .0108$) of E0771 cells (Figures 1F and 1G), and reshaped their immunity gene expression (Supplementary Methods; Figure 1H) up-regulating inflammatory mediators, such as *Il1 β* , *Il4*, *Il5*, *Il17a*, *Csf3*, *Egf*, *Il23*, *Il22*, *Ccl28* and chemokine receptors, especially, *Ccr4*, *Cxcr5*, *Cxcr2*, and *Cxcr3*, which promote invasive migration of cancer cells.⁸ IL30 also upregulated *Ptgs2*, *Ido1*, *Cd274/Pd-l1*, *B7h4*, and *Lag3*,⁹ which mediate tumor immune escape, along with *Bcl2l1*, *Myc*, *Trp53*, *Klf4*, *Bmi1*, and, especially, *Snai2*, which fosters tumor progression.¹⁰

The tumor-promoting effects on TNBC cells endowed with the IL30R, led us to speculate that targeting IL30 might inhibit IL30-responsive tumors. However, when orthotopically implanted into *IL30KO* mice, both IL30-responsive and unresponsive TNBC cell lines gave rise to tumors that grew slower (Student's *t*-test, $P < .01$) than in WT mice, and reached, 18 and 40 days later, respectively, a mean tumor volume (MTV) that was lower than that of WT mice (E0771 tumors: $309 \pm 194 \text{ mm}^3$ in *IL30KO* versus $1342 \pm 137 \text{ mm}^3$ in WT; AT-3 tumors: $580 \pm 199 \text{ mm}^3$ in *IL30KO* versus $1257 \pm 145 \text{ mm}^3$ in WT; Student's *t*-test: $P = .00005$ and $P = .0020$, respectively; Figures 1I and 1J). In both experiments, the survival of tumor-bearing *IL30KO* mice was considerably longer (log rank test: $P < .05$; Figures 1K and 1L).

This is an open access article under the terms of the [Creative Commons Attribution](https://creativecommons.org/licenses/by/4.0/) License, which permits use, distribution and reproduction in any medium, provided the original work is properly cited.

© 2021 The Authors. *Clinical and Translational Medicine* published by John Wiley & Sons Australia, Ltd on behalf of Shanghai Institute of Clinical Bioinformatics

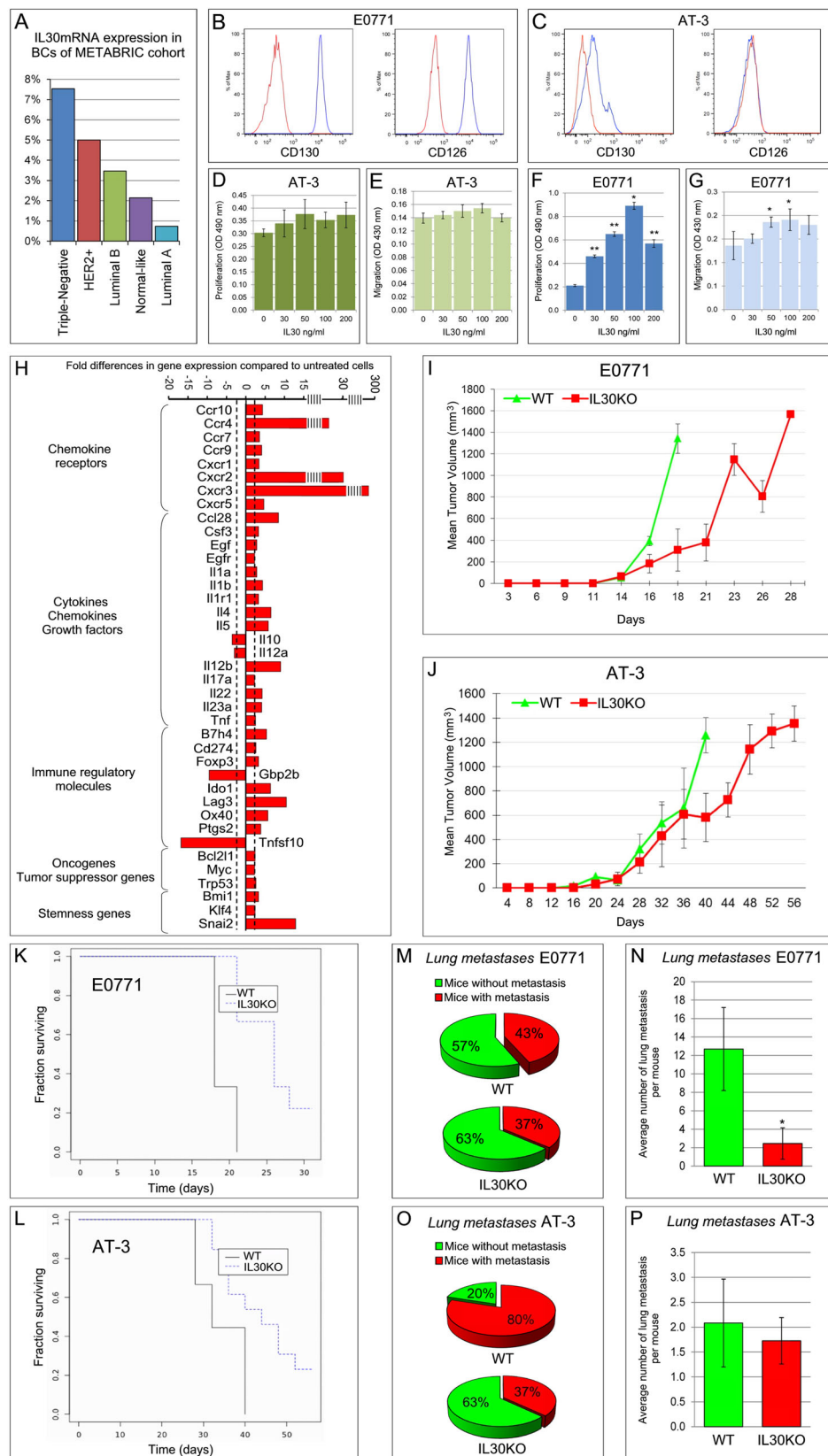


FIGURE 1 IL30 expression in human TNBC and effects of IL30 on murine TNBC cell lines in vitro and in vivo. A, IL30mRNA expression in human BC subtypes from the METABRIC cohort. The histogram represents the percentage of IL30 over-expressing cases (Z-score > 2) out of the total number of cases for each BC subtype. B and C, Cytofluorimetric analyses of gp130 (CD130) and IL6R α (CD126) expression in E0771

Among E0771 tumor-bearing mice, the number of *IL30KO* mice, which developed lung metastasis (11/30; 37%) was comparable to that of WT mice (13/30, 43%) (Figure 1M), however the average number of metastasis per mouse was lower in *IL30KO* mice (3 versus 13) (Student's *t*-test: $P = .004$; Figure 1N).

Among AT-3 tumor-bearing mice, only 11 out of 30 (37%) of *IL30KO* mice developed lung metastasis versus 24 out of 30 (80%) of WT mice (Fisher Exact Test: $P = .0014$; Figure 1O), whereas no difference in the average number of metastases per mouse was found between the two groups (Figure 1P).

In WT mice, both E0771 and AT-3 tumors were well vascularized and infiltrated by IL30 expressing leukocytes, mostly MDCs and macrophages, that were lacking in tumors developed in *IL30KO* mice (Supplementary Methods and Tables S1 and S2; Figures 2A-2E). The absence of EB13 excluded IL27 production in the microenvironment (Figure S2). In *IL30KO* mice, both types of tumors were poorly vascularized with necrotic-hemorrhagic features, whereas only E0771 tumors showed a lower proliferation index (Figures 2A-2C; Table S2). In *IL30KO* mice, both tumor models revealed a scanty CD11b⁺Gr-1⁺MDC and F4/80⁺macrophage infiltrate, and a reduced CD4⁺Foxp3⁺T regulatory cell content, whereas CD4⁺T, CD8⁺T, and NKp46⁺ cells were increased when compared with controls (Figures 2D and 2E).

IFN γ expression was found in tumors, LNs and spleens of tumor-bearing *IL30KO* mice and largely co-localized with CD3⁺T lymphocytes (Figures 2B, 2F and 2G; Figures S3A and S3B, and Table S3), although the contribution of myeloid cells cannot be completely excluded. Specifi-

cally, CD3⁺CD8⁺, CD3⁺CD4⁺, and CD3⁻NKp46⁺ cells, to a lesser extent, were the source of IFN γ production in the tumor microenvironment (Figures 3A and 3B).

To investigate the role of IFN γ in the anti-tumor effects due to the lack of IL30, we generated *IL30/IFN γ KO* mice (Supplementary Methods and Figure S4A, S4B, and S4C) and selectively blocked, in *IL30KO* mice, IFN γ pathway with neutralizing anti-IFN γ Abs.

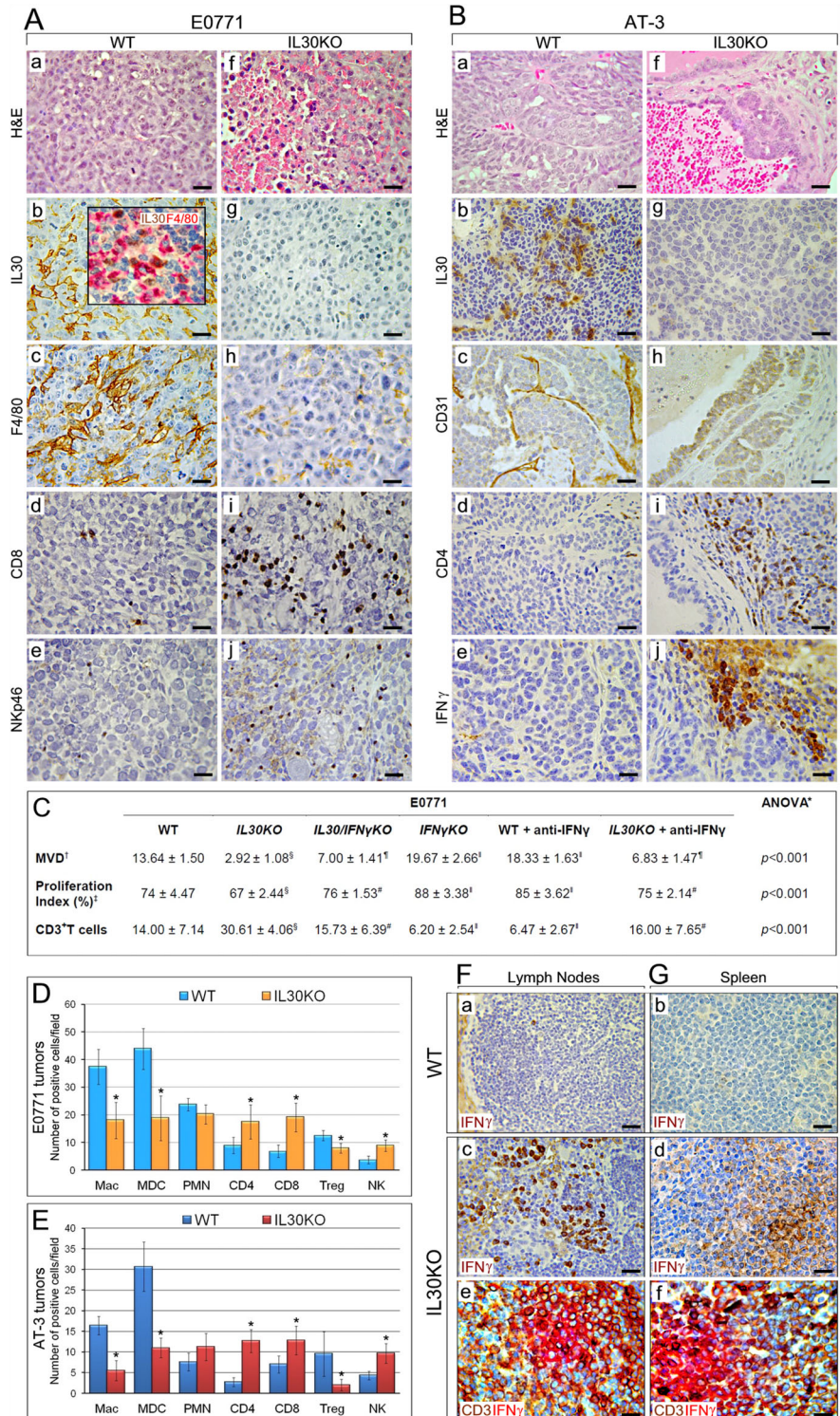
The growth of both TNBCs was restored in *IL30/IFN γ KO* or in *IL30KO* hosts in which the IFN γ pathway was blocked.

In *IL30/IFN γ KO* hosts, E0771 and AT-3 cells gave rise to tumors that reached a MTV of 1470 ± 88 and 1073 ± 135 mm³, respectively, that was significantly higher (ANOVA: $P < .001$; Tukey HSD Test: $P < .01$) than that of tumors developed in *IL30KO* mice and comparable to that of control tumors in WT mice (Figures 3C and 3D). The proliferation index of tumors developed in *IL30/IFN γ KO* mice was comparable to control tumors. In both E0771 and AT-3 tumors, which developed in *IL30/IFN γ KO* mice, the microvessel density was higher (ANOVA: $P < .001$; Tukey HSD Test: $P < .01$) than in tumors developed in *IL30KO* mice, and comparable to control tumors. By contrast, CD3⁺T lymphocytes were drastically reduced when compared with tumors developed in *IL30KO* (ANOVA: $P < .001$; Tukey HSD Test: $P < .01$) and comparable to control tumors (Table S2; Figures 2C, 3E, and 3F). Thereby, abrogation of IFN γ signaling enhances tumor vascularization and prevents the intra-tumoral influx of T lymphocytes.¹¹

IFN γ , evaluated by flow cytometry (Supplementary Methods), was absent in tumors developed in

(B) and in AT-3 cells (C). Blue profiles: specific markers; red profiles: isotype controls. Experiments were performed in triplicate. D, MTT assay of AT-3 cells, 48 hours after rmIL30 treatment. Data are representative of three independent experiments. Results are expressed as mean \pm SD. ANOVA: $P = .315$. E, Number of migrating and invading AT-3 cells, 48 hours after rmIL30 treatment. Results are expressed as mean \pm SD. ANOVA: $P = .118$. F, MTT assay of E0771 cells, 48 hours after rmIL30 treatment. Data are representative of three independent experiments. Results are expressed as mean \pm SD. ANOVA: $P < .001$. * $P < .05$, Tukey HSD Test compared with 0, 30, 50, and 200 ng/mL. ** $P < .05$, Tukey HSD Test compared with 0 ng/mL. G, Number of migrating and invading E0771 cells, 48 hours after rmIL30 treatment. Results are expressed as mean \pm SD. ANOVA: $P = .011$. * $P < .05$, Tukey HSD Test compared with 0 ng/mL. H, Cancer inflammation and immunity crosstalk PCR Array reveals the fold differences of individual mRNAs between E0771 cells treated and untreated with rmIL30 (red bars). Pooled results \pm SD are from two experiments performed in duplicate. A significant threshold of a two-fold change in gene expression corresponded to a $P < .001$. I and J, Mean volume of tumors developed after orthotopic implantation of E0771 (I) and AT-3 cells (J) in WT or in *IL30KO* mice. Student's *t*-test: $P < .01$ versus WT mice. Results from *B6 EIIa-cre* mice and *p28^{f/f}* mice were comparable to those obtained in WT mice (Fisher Exact Probability Test: $P > .99$). K and L, Kaplan-Meier survival curves of E0771 (K) and AT-3 (L) tumor bearing WT and *IL30KO* mice. Log-rank test: $P = .0014$ (K) and $.012$ (L). M, Percentage of WT and *IL30KO* mice, bearing E0771 tumors, with (red) and without (green) lung metastasis. Fisher Exact Probability Test: $P = .792$. N, Average number of lung metastasis per mouse developed in WT and *IL30KO* mice bearing E0771 tumors. * $P = .004$, Student's *t*-test compared with WT mice. The number of metastases per mouse did not correlate with the tumor size, as determined by Pearson correlation coefficient ($r = .002$). O, Percentage of WT and *IL30KO* mice, bearing AT-3 tumors, with (red) and without (green) lung metastasis. Fisher Exact Probability Test: $P = .0014$. The number of mice which developed metastasis did not correlate with the tumor size, as determined by Spearman's rank correlation coefficient ($\rho = .203$). P, Average number of lung metastasis per mouse developed in WT and *IL30KO* mice bearing AT-3 tumors. Student's *t*-test: $P = .129$

FIGURE 2 Immuno-pathological features of TNBCs developed in *IL30KO* mice. A and B, Hematoxylin and Eosin (H&E) stained sections and immunohistochemical characterization of E0771 tumors (A) and AT-3 tumors (B) developed in WT (a, b, c, d, e) and in *IL30KO* (f, g, h, i, j) mice. Magnification: X400. Scale bars: 30 μm . C, Microvessel density (MVD), proliferation, and T lymphocyte infiltration of E0771 tumors. *One-way ANOVA for comparisons between the six mouse groups. \dagger MVD: mean \pm SD of CD31 positive vessels/field (85431.59 μm^2). \ddagger Proliferation Index (%): mean percentage \pm SD of PCNA positive cells/number of total cells per field (85431.59 μm^2). $\S P < .01$, Tukey HSD Test compared with tumors in WT, *IL30/IFN γ KO*, *IFN γ KO*, WT + anti-IFN γ Abs and *IL30KO* + anti-IFN γ Abs. $\parallel P < .01$, Tukey HSD Test compared with tumors in WT, *IL30KO*, *IFN γ KO*, and WT + anti-IFN γ Abs. $\# P < .01$, Tukey HSD Test compared with tumors in *IL30KO*, *IFN γ KO*, and WT + anti-IFN γ Abs. $\|\ P < .01$, Tukey HSD Test compared with tumors in WT, *IL30KO*, *IL30/IFN γ KO*, and *IL30KO* + anti-IFN γ Abs. D and E, Immune cell counts in E0771 (D) and AT-3 (E) tumors developed in WT and in *IL30KO* mice. Results are expressed as mean \pm SD of positive cells/field evaluated at X400 (85431.59 μm^2 field) by immunohistochemistry. * $P < .01$, Student's *t*-test compared with tumors in WT mice. F and G, Immunohistochemical detection of IFN γ (brown) in tumor draining lymph nodes (a, c, e) and in the spleen (b, d, f) of E0771 tumor bearing WT (a, b) and *IL30KO* (c, d, e, f) mice. The double staining reveals the frequent co-localization (brick color) of IFN γ (red) with CD3 $^+$ T cells (brown), both in the lymph nodes (e) and spleen (f) of E0771 tumor bearing *IL30KO* mice. Magnification: X400. Scale bars: 30 μm



IL30/IFN γ KO and *IFN γ KO* mice (Figures 3G and 3H), whereas it was produced by CD3 $^+$ CD4 $^+$, CD3 $^+$ CD8 $^+$, and CD3 $^-$ NKp46 $^+$ cells infiltrating tumors developed in *IL30KO* mice (Figure 3I).

The growth, vascularization, and T lymphocyte content of both E0771 and AT-3 tumors, developed in *IL30KO* mice treated with anti-IFN γ Abs, were comparable to those

observed in *IL30/IFN γ KO* mice (MTV of E0771 tumors: Tukey HSD Test: $P = .18$; MTV of AT-3 tumors: Tukey HSD Test: $P = .90$; Figures 2C, 3C, and 3D; Table S2).

Overall, the lack of endogenous IL30 triggers IFN γ production by T and NK cells, hinders TNBC progression and leads to improved survival. This study consolidates our recent findings¹² and provides the proof of concept that

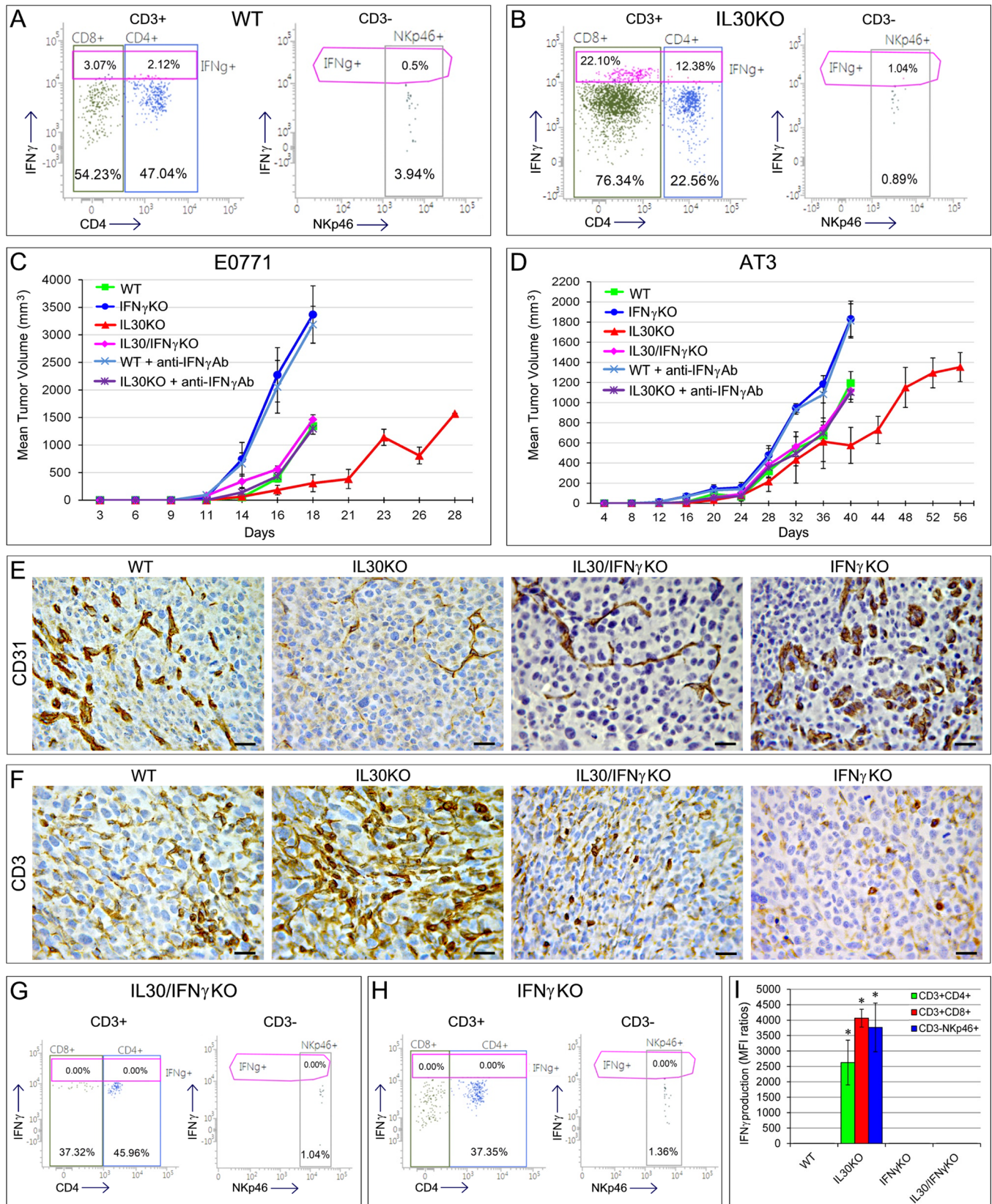


FIGURE 3 Growth curves and immuno-pathological features of TNBCs developed in *IL30KO*, *IFN_γKO*, *IL30/IFN_γKO* mice, and in WT or *IL30KO* mice treated with neutralizing anti-IFN_γ Abs. A and B, Flow cytometry analysis of IFN_γ production, by tumor infiltrating cells, in two representative tumors developed in WT (A) and *IL30KO* (B) mice injected with E0771 cells. After exclusion of dead cells (7-AAD⁺), CD3⁺CD4⁺ (blue), CD3⁺CD8⁺ (green), and CD3⁻NKp46⁺ (grey) nucleated cells were gated and analyzed for IFN_γ expression (purple). The percentages of CD4⁺ cells and CD8⁺ cells of parent CD3⁺ population, percentage of NKp46⁺ cells of CD3⁻ parent population and percentage of

IL30 is a valuable target to improve immunotherapy and life expectancy in TNBC patients.

ACKNOWLEDGMENTS

This work was supported by AIRC (IG 2019 - ID. 23264, P.I. Emma Di Carlo) and the Italian Ministry of Health (Ricerca Finalizzata, RF-2013-02357552 and RF-2016-02362022).

CONFLICT OF INTEREST

The authors declare that there is no conflict of interest that could be perceived as prejudicing the impartiality of the research reported.

ETHICS APPROVAL AND CONSENT TO PARTICIPATE

Animal procedures were performed in accordance with the European Community guidelines and approved by the Institutional Animal Care Committee of "G. d'Annunzio" University and the Italian Ministry of Health (authorization number: 892/2018-PR).

AUTHOR CONTRIBUTIONS


Emma Di Carlo was responsible for the study design and supervision and wrote the paper; Carlo Sorrentino, Stefania Livia Ciummo, Luigi D'Antonio, Paola Lanuti performed the experiments; Emma Di Carlo, Carlo Sorrentino, Stefania Livia Ciummo performed data analysis; Li-Fan Lu and Zhinan Yin provided *IL30KO* mice; Scott I. Abrams provided the AT-3 cell line; and all authors approved the final version of the manuscript.

CONSENT FOR PUBLICATION

All authors have read the manuscript and approved its submission to *Clinical and Translational Medicine*.

DATA AVAILABILITY STATEMENT

The data that support the findings of this study are available from Emma Di Carlo upon reasonable request.

Carlo Sorrentino^{1,2}
 Stefania Livia Ciummo^{1,2}
 Luigi D'Antonio^{1,2}
 Paola Lanuti¹
 Scott I. Abrams³
 Zhinan Yin⁴
 Li-Fan Lu⁵
 Emma Di Carlo^{1,2} 

¹ Department of Medicine and Sciences of Aging, "G. d'Annunzio" University, Chieti, Italy

² Anatomic Pathology and Immuno-Oncology Unit, Center for Advanced Studies and Technology (CAST), "G. d'Annunzio" University, Chieti, Italy

³ Department of Immunology, Roswell Park Cancer Institute (RPCI), Buffalo, New York, USA

⁴ The First Affiliated Hospital, Biomedical Translational Research Institute, Guangdong Province Key Laboratory of Molecular Immunology and Antibody Engineering, Jinan University, Guangzhou, China

⁵ Division of Biological Sciences, Center for Microbiome Innovation and Moores Cancer Center, University of California, San Diego, California, USA

IFN γ ⁺ cells are reported. Isotype controls were used to assess the background, and experiments were performed in triplicate. C and D, Mean volume of tumors (MTV) developed after orthotopic implantation of E0771 (C) and AT-3 (D) cell lines in *IL30/IFN γ KO* mice, *IFN γ KO* mice, *IL30KO* mice, WT mice, and WT or *IL30KO* mice treated with anti-IFN γ Abs. ANOVA: $P < .0001$. Tukey's HSD test: $P < .01$ (*IFN γ KO* mice and WT mice treated with anti-IFN γ Abs versus *IL30KO*, *IL30/IFN γ KO*, *IL30KO* mice treated with anti-IFN γ Abs and WT mice; *IL30KO* mice versus *IFN γ KO* mice, WT mice treated with anti-IFN γ , *IL30/IFN γ KO* mice, *IL30KO* mice treated with anti-IFN γ Abs and WT mice). The growth curves of both E0771 and AT-3 tumors, developed in *IL30KO* mice treated with anti-IFN γ Abs, were comparable to those observed in *IL30/IFN γ KO* mice (MTV of E0771 tumors in *IL30KO* mice treated with anti-IFN γ Abs: 1298.59 ± 103.54 mm³; MTV of E0771 tumors in *IL30/IFN γ KO* mice: 1464.16 ± 87.34 mm³; Tukey HSD Test: $P = .18$. MTV of AT-3 tumors in *IL30KO* mice treated with anti-IFN γ Abs: 1103.23 ± 98.46 mm³; MTV of AT-3 tumors in *IL30/IFN γ KO* mice: 1118.30 ± 85.98 mm³; Tukey HSD Test: $P = .90$). The growth of tumors in WT mice treated with anti-IFN γ Abs was comparable to that observed in *IFN γ KO* mice (MTV of E0771 tumors in WT mice treated with anti-IFN γ Abs: 3186.89 ± 333.71 mm³; MTV of E0771 tumors in *IFN γ KO* mice: 3369.92 ± 520.94 mm³; Tukey HSD Test: $P = .10$. MTV of AT-3 tumors in WT mice treated with anti-IFN γ Abs: 1811.37 ± 169.94 mm³; MTV of AT-3 tumors in *IFN γ KO* mice: 1831.85 ± 176.00 mm³; Tukey HSD Test: $P = .90$). E, The vascular network of E0771 tumors developed in WT (a), *IL30KO* (b), *IL30/IFN γ KO* (c), and *IFN γ KO* (d) mice, as assessed by CD31 immunostaining. Magnification: X400. Scale bars: 30 μ m. F, T lymphocyte infiltrate in E0771 tumors developed in WT (a), *IL30KO* (b), *IL30/IFN γ KO* (c), and *IFN γ KO* (d) mice, as assessed by CD3 immunostaining. Magnification: X400. Scale bars: 30 μ m. G and H, Flow cytometry analysis of IFN γ production, by tumor infiltrating cells, in two representative tumors developed in *IFN γ KO* and *IL30/IFN γ KO* mice, shows the absence of IFN γ in tumor infiltrating CD3⁺CD4⁺, CD3⁺CD8⁺, and CD3⁻NKp46⁺ cells. The percentages of CD4⁺ cells and CD8⁺ cells of parent CD3⁺ population, percentage of NKp46⁺ cells of CD3⁻ parent population, and percentage of IFN γ ⁺ cells are reported. Isotype controls were used to assess the background and experiments were performed in triplicate. I, The production of IFN γ , measured as mean fluorescence intensity (MFI) ratios, detected in CD3⁺CD4⁺, CD3⁺CD8⁺, and CD3⁻NKp46⁺ cells infiltrating the tumors developed in WT, *IL30KO*, *IFN γ KO*, and *IL30/IFN γ KO* mice. MFI ratios were calculated by dividing the MFI of IFN γ ⁺ cell population by the MFI of the negative/isotype control. Five tumor samples per experimental group were examined

Correspondence

Emma Di Carlo, Anatomic Pathology and
Immuno-Oncology Unit, Center for Advanced Studies
and Technology (CAST), “G. d’Annunzio” University, Via
L. Polacchi 11, 66100, Chieti, Italy.
Email: edicarlo@unich.it

Carlo Sorrentino and Stefania Livia Ciummo contributed
equally to this work.

KEYWORDS

IFN γ , interleukin-30, triple negative breast cancer, tumor microenvironment

ORCID

Emma Di Carlo  <https://orcid.org/0000-0001-7778-1042>

REFERENCES

1. Di Meo S, Airoidi I, Sorrentino C, Zorzoli A, Esposito S, Di Carlo E. Interleukin-30 expression in prostate cancer and its draining lymph nodes correlates with advanced grade and stage. *Clin Cancer Res.* 2014;20:585-594.
2. Sorrentino C, Ciummo SL, Cipollone G, Caputo S, Bellone M, Di Carlo E. Interleukin-30/IL27p28 shapes prostate cancer stem-like cell behavior and is critical for tumor onset and metastasization. *Cancer Res.* 2018;78:2654-2668.
3. Airoidi I, Cocco C, Sorrentino C, et al. Interleukin-30 promotes breast cancer growth and progression. *Cancer Res.* 2016;76:6218-6229.
4. Pflanz S, Timans JC, Cheung J, et al. IL-27, a heterodimeric cytokine composed of EBI3 and p28 protein, induces proliferation of naive CD4+ T cells. *Immunity.* 2002;16:779-790.
5. Garbers C, Spudy B, Aparicio-Siegmund S, et al. An interleukin-6 receptor-dependent molecular switch mediates signal transduction of the IL-27 cytokine subunit p28 (IL-30) via a gp130 protein receptor homodimer. *J Biol Chem.* 2013;288:4346-4354.
6. Ferlay J, Colombet M, Soerjomataram I, et al. Estimating the global cancer incidence and mortality in 2018: GLOBOCAN sources and methods. *Int J Cancer.* 2019;144:1941-1953.
7. Zhang S, Liang R, Luo W, et al. High susceptibility to liver injury in IL-27 p28 conditional knockout mice involves intrinsic interferon- γ dysregulation of CD4+ T cells. *Hepatology.* 2013;57:1620-1631.
8. Müller A, Homey B, Soto H, et al. Involvement of chemokine receptors in breast cancer metastasis. *Nature.* 2001;410:50-56.
9. Ruffo E, Wu RC, Bruno TC, Workman CJ, Vignali DAA. Lymphocyte-activation gene 3 (LAG3): the next immune checkpoint receptor. *Semin Immunol.* 2019;42:101305.
10. Ferrari-Amorotti G, Chiodoni C, Shen F, et al. Suppression of invasion and metastasis of triple-negative breast cancer lines by pharmacological or genetic inhibition of slug activity. *Neoplasia.* 2014;16:1047-1058.
11. Nakajima C, Uekusa Y, Iwasaki M, et al. A role of interferon-gamma (IFN-gamma) in tumor immunity: t cells with the capacity to reject tumor cells are generated but fail to migrate to tumor sites in IFN-gamma-deficient mice. *Cancer Res.* 2001;61:3399-3405.
12. Sorrentino C, Yin Z, Ciummo S, et al. Targeting interleukin (IL)-30/IL-27p28 signaling in cancer stem-like cells and host environment synergistically inhibits prostate cancer growth and improves survival. *J Immunother Cancer.* 2019;7:201.

SUPPORTING INFORMATION

Additional supporting information may be found online in the Supporting Information section at the end of the article.